1-1-2014

Large scale production of novel g-C3N4 micro strings with high surface area and versatile photodegradation ability

Muhammad Nawaz Tahir
Beijing Institute of Technology

Chuanbao Cao
Beijing Institute of Technology

Faheem K. Butt
Beijing Institution Of Technology

Sajid Butt
Tsinghua University

Faryal Idrees
Beijing Institution Of Technology

See next page for additional authors

Recommended Citation

Large scale production of novel g-C3N4 micro strings with high surface area and versatile photodegradation ability

Abstract

An easy, scalable and environmentally benign chemical method has been developed to synthesize micro strings of graphitic-C3N4 (msg-C3N4) through pre-treatment of melamine with HNO 3 in alkaline solvent at low temperature. This methodology results in a unique string type morphology of msg-C3N4 with higher surface area. These msg-C3N4 micro strings were used as a photocatalyst under visible light for photodegradation of rhodamine B, methyl blue and methyl orange. The msg-C3N4 shows enhanced photodegradation efficiency due to its high surface area and favourable bandgap. The first order rate constant for msg-C3N4 was measured which confirms the higher performance of msg-C3N4 in comparison to other reported materials such as g-C3N4, Fe2O3/g-C3N4 and TiO2 nanotubes. Thus, the method developed here is favourable for the synthesis of materials with higher surface area and unique morphology, which are favourable for high photodegradation activity. The Royal Society of Chemistry.

Keywords

scale, large, c, inf, 3, production, novel, g, n, 4, ability, micro, strings, photodegradation, versatile, area, surface, high

Disciplines

Engineering | Physical Sciences and Mathematics

Authors

Muhammad Nawaz Tahir, Chuanbao Cao, Faheem K. Butt, Sajid Butt, Faryal Idrees, Zulfiqar Ali, Imran Aslam, M Tanveer, Asif Mahmood, and Nasir Mahmood

Large scale production of novel g-C$_3$N$_4$ micro strings with high surface area and versatile photodegradation ability†

Muhammad Tahir,[a] Chuanbao Cao,*[a] Faheem K. Butt,[a] Sajid Butt,[b] Faryal Idrees,[a] Zulfiqar Ali,[a] Imran Aslam,[a] M. Tanveer,[a] Asif Mahmood[c] and Nasir Mahmood[c]

An easy, scalable and environmentally benign chemical method has been developed to synthesize micro strings of graphitic-C$_3$N$_4$ (msg-C$_3$N$_4$) through pre-treatment of melamine with HNO$_3$ in alkaline solvent at low temperature. This methodology results in a unique string type morphology of msg-C$_3$N$_4$ with higher surface area. These msg-C$_3$N$_4$ micro strings were used as a photocatalyst under visible light for photodegradation of rhodamine B, methyl blue and methyl orange. The msg-C$_3$N$_4$ shows enhanced photodegradation efficiency due to its high surface area and favourable bandgap. The first order rate constant for msg-C$_3$N$_4$ was measured which confirms the higher performance of msg-C$_3$N$_4$ in comparison to other reported materials such as g-C$_3$N$_4$, Fe$_2$O$_3$/g-C$_3$N$_4$ and TiO$_2$ nanotubes. Thus, the method developed here is favourable for the synthesis of materials with higher surface area and unique morphology, which are favourable for high photodegradation activity.

Introduction

Environmental problems have been increasing at exponential rates in recent years due to global warming. A lot of research has been devoted to solve these concerns. One of the approaches to solve these issues is to make use of sunlight for decomposing harmful chemicals present in the environment. Harvesting solar energy is very important in the context of solving environmental issues as the source is always emitting energy at a high rate and energy is available around the globe. This energy can be efficiently utilized using species that can convert solar energy into applicable form.

The search for optimized and highly efficient photocatalysts is highly needed to deal with environmental concerns. Photocatalysis is used to remove pollutants through photo-oxidation in the presence of light and photocatalyst.[1,2] These nano-robots or nano-sweepers require strong oxidative ability, a suitable bandgap and excellent stability in water solution.

[a] *Research Center of Materials Science, Beijing Institute of Technology, Beijing 100081, People's Republic of China. E-mail: cbcao@bit.edu.cn; Fax: +86 10 6891 2001; Tel: +86 10 6891 3792*
[b] *School of Materials Science and Engineering Tsinghua University, Beijing 100081, People's Republic of China*
[c] *Department of Materials Science and Engineering, Peking University, Beijing 100081, PR China*
† Electronic supplementary information (ESI) available: SEM and XRD of growth mechanism, digital photograph of msg-C$_3$N$_4$, C/C_0 of RhB, k value of RhB with different concentration and efficiency of msg-C$_3$N$_4$ can be found in ESI. See DOI: 10.1039/c3ce42135j

Various semiconductors have been proposed as photocatalysts during recent decades, such as metal oxides, sulphides and oxy-nitrides.[3,4] Among them, numerous metal (Ag, Au, Pt and Pd) nanostructures have shown good photocatalytic response due to their large surface area but have some issues due to agglomeration and stability over a period of time.[5] Consequently, new photocatalysts that are stable, efficient, inexpensive, non-toxic and capable of harvesting sunlight are highly desirable.

Graphitic carbon nitride (g-C$_3$N$_4$) is a promising material with excellent mechanical and thermal properties, a catalyst for organic synthesis, a photoelectric converter, an electrode material for fuel cells or batteries, a hydrogen storage material and a fluorescent sensor.[6–8] g-C$_3$N$_4$, a metal free catalyst, has been investigated as an environmentally friendly photocatalyst for photodegradation of organic pollutants in water.[8,9] Fast recombination of photogenerated charge carriers and the low surface area of g-C$_3$N$_4$ limits the search for high efficiency. Thus, various attempts have been made to solve these problems, *e.g.* doping with heteroatoms, tuning compositions, coupling with other semiconductors and preparation of nano or porous g-C$_3$N$_4$.[9–20]

The morphology, size, shape, dimension and surface area of nanostructures are key features for photocatalytic activities.[21–26] Unfortunately the surface areas of g-C$_3$N$_4$ fabricated from precursors such as melamine, cyanamide and dicyanamide are very small (~15 m^2 g^{-1}).[27] In order to achieve high surface area several template methods have been investigated, for example Xu *et al.* fabricated g-C$_3$N$_4$ with a surface

area of 128 m^2 g^{-1}, Wang *et al.* synthesized g-C_3N_4 with a high surface area of 239 m^2 g^{-1} and Yuliati *et al.* also synthesized g-C_3N_4 with a surface area of224 m^2 g^{-1}.[27–34] The resultant g-C_3N_4 showed superior photocatalytic activities toward photodegradation or hydrogen production but their practical application was limited since the template was removed by HF, which poisoned the product. Elimination of the template removal process could increase practical application of the material. Designing a specific morphology also gives enhanced properties to the product *e.g.* string-like structures have advantages of large aspect ratio, low density, good chemical and environmental stability. Moreover, the string-like morphology also had advantages over nanowires and nanotubes in lithiation and de-lithiation processes in lithium ion batteries.[33] Thus, an easy and scalable method is required to prepare g-C_3N_4 with high surface area and specific morphology without using templates and toxic chemicals to make its application more practical in the fields of catalysis and energy storage.

Here, we report a large scale, controlled synthesis of g-C_3N_4 micro strings by pre-treatment of melamine with HNO_3. To the best of our knowledge these strings have not been reported yet and the methodology developed is easy, economical, works at low temperature and is template free. In order to study the possible growth mechanism of msg-C_3N_4, time-dependent experiments were performed and appropriate conditions were defined. Moreover, the effects of the solvent and HNO_3 on the morphology of msg-C_3N_4 were also explored. The msg-C_3N_4 was used as a photocatalyst for rhodamine B (RhB), methyl blue (MB) and methyl orange (MO) degradation under visible light. Results suggest improved photocatalytic performance without considerable loss of efficiency upon recycling. Therefore, by using current methodology, higher surface area and novel morphology can be achieved simultaneously, which are favorable for high photocatalytic activity.

Experimental section

Preparation of msg-C_3N_4

1 g melamine was dissolved in 20 ml of ethylene glycol with continuous stirring, followed by addition of 60 ml of 0.2 M HNO_3 solution. The resultant mixture was stirred for 10 minutes. Finally, the product was washed with ethanol and dried at 80 °C. After drying, the obtained white powder was annealed at 400 °C for 2 h in a muffle furnace in alumina crucibles. After annealing, a yellowish powder was collected and stored for characterization. In addition, bulk g-C_3N_4 was also prepared according to the literature.[9] Sample was characterized by scanning electron microscopy (SEM), transmission electron microscopy (TEM), selected-area electron diffraction (SAED), X-ray diffraction (XRD), X-ray photoelectron spectroscopy (XPS) and photoluminescence absorption spectroscopy (PL).

Photocatalytic test

For photocatalytic tests, a certain amount of sample was dissolved in 40 ml aqueous solutions of RhB, MB or MO in glass beakers. The concentration of RhB, MB and MO was 10 mg in 1 L of H_2O. At first, the solution was stirred continuously in the dark for 30 minutes to establish adsorption–desorption equilibrium among the photocatalysts and dye solution, then this solution was brought into visible light. A 500 W xenon lamp was used as a visible light source and the glass beaker was placed in front of the lamp during continuous magnetic stirring. 3 ml of solution was taken and UV absorption measurements were used to observe the photodegradation at specific time intervals. Every time before measuring UV, the solution was centrifuged to remove the suspension particles of the catalyst. The absorption peaks for RhB, MB and MO were observed at 554, 610 and 465 nm respectively. For stability measurements the same materials were taken from the solution and the above mentioned steps were repeated for second and third times.

Results and discussion

Characterization of the msg-C_3N_4

X-ray diffraction (XRD) study was performed in order to investigate the crystal structure and phase of the as-prepared samples. Two distinctive XRD peaks were observed for g-C_3N_4 at 27.5° and 13.1° as shown in Fig. 1(a). The strong peak at 27.5° corresponds to the long-range inter-planar stacking of aromatic systems with an inter-planar distance of 0.324 nm. The small peak at 13.1° (100) is related to d = 0.76 nm because of in-plane structural packing motif. However, there is only one broad peak at 27.3° for msg-C_3N_4 resembling that at 27.5° for g-C_3N_4 related to (002), showing that the msg-C_3N_4 peak is slightly shifted and its corresponding

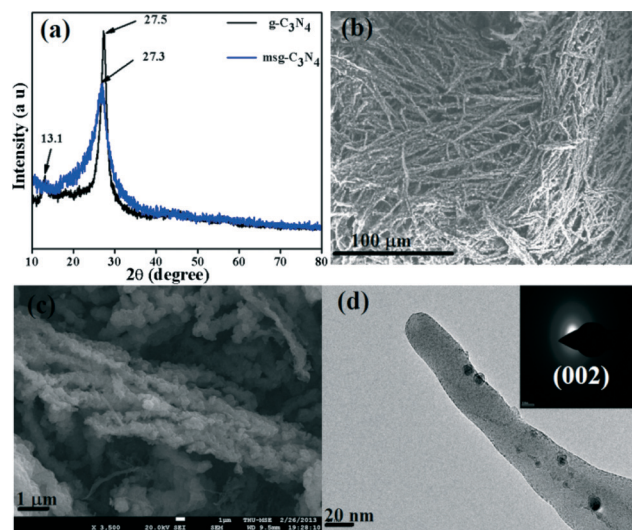**Fig. 1** (a) XRD patterns of msg-C_3N_4 and g-C_3N_4; (b) low and (c) high magnification SEM images of msg-C_3N_4; (d) TEM image and SAED pattern (inset) of msg-C_3N_4.

inter-planer distance 0.326 nm is increased as compared to g-C_3N_4.[35–37]

The morphology and microstructures of msg-C_3N_4 were characterized through SEM and TEM as shown in Fig. 1(b–d). From Fig. 1(b), it is obvious that as-prepared micro strings are uniform and dense without aggregation. These msg-C_3N_4 have an aspect ratio of 50, as their length is in the range of tens of microns and their diameter is 2–4 micrometers. From Fig. 1(b), it is obvious that as-synthesized msg-C_3N_4 has a well-defined string structure with large accommodation sites for host species as shown in Fig. 1(c). Furthermore, the TEM image delineated in Fig. 1(d) confirmed growth of the strings with uniform dimensions. SAED studies were carried out (inset of Fig. 1d) to further confirm the structure of msg-C_3N_4. Thus, the diffraction ring indexed as (002) is in accordance with the XRD result (Fig. 1(d)) with d = 0.33 nm.

In order to probe the chemical compositions and chemical states of the msg-C_3N_4, XPS characterization was performed as shown in Fig. 2. The C1s spectrum has two peaks at 288.15 eV and 284.6 eV, which are attributed to the existence of C–N–C coordination and surface adventitious carbon, respectively, as shown in Fig. 2(a).[37] Similarly, the N1s spectra of msg-C_3N_4 has three peaks at 398.8, 399.4 and at 400.3 eV, which correspond to pyridinic, amino and pyrrolic nitrogen centres, respectively. The C/N ratio of msg-C_3N_4 calculated using XPS is 0.82, a little higher in comparison with the theoretical value of 0.75, which proves that msg-C_3N_4 has a low concentration of N. In order to study the growth mechanism of msg-C_3N_4, time-dependent experiments were performed and appropriate conditions were optimized. In this context, melamine was treated with HNO_3 and the mixture was calcined. For growth studies, products were collected and studied at different time intervals (60, 90, 120, 150 minutes) during the calcination process. It is obvious that melamine particles (Fig. 3(a)) were converted into rod type structures (Fig. 3(b)) as a result of calcination for first 60 minutes. Product collected after 90 minutes suggests the destruction of rods and formation of small beads (Fig. 3(c)). Prolonged calcination up to 120 minutes leads to fusion of these beads and formation of small string type structures (Fig. 3(d)). Further increase in exposure time up to 150 minutes at the same temperature leads to fusion of stray strings together and formation of long micro strings with high aspect ratio, as shown in Fig. 3(d–e). The presence of
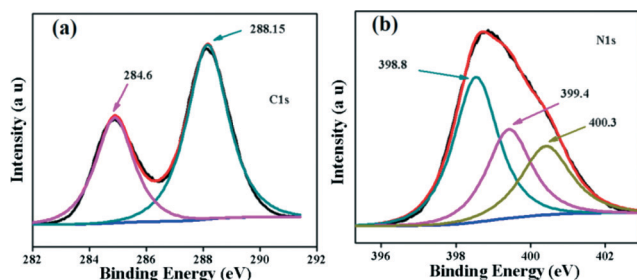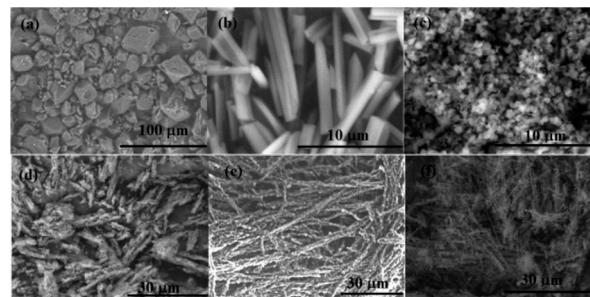

Fig. 3 SEM images of (a) melamine, (b) nanorods, (c) msg-C_3N_4 after 60 minutes, (d) msg-C_3N_4 after 90 minutes, (e) msg-C_3N_4 after 120 minutes, (f) msg-C_3N_4 after 150 minutes.

small beads on the surface of these strings is also obvious, which suggests further growth of these micro strings in the case of the presence of more reactive species. SEM images of the intermediate and final products without HNO_3 and ethylene glycol are also given in Fig. S3†.

XRD patterns of melamine and msg-C_3N_4 heated at different time periods are presented in Fig. S4†. The XRD patterns of rods and melamine are different from each other, which confirms the advantages of pre-treatment of melamine with HNO_3, which converts melamine to nanoparticles as shown in Fig. S3.† The other samples are identified as g-(002) with peak positions 26.5°, 26.9°, 27.3° and 27.5° after 60, 90, 120 and 150 minutes, respectively. The intensity of the peak also increases with time, which indicates enhancement in the quality and stability of the crystal structure, but a longer time period (150 minutes) destroy the string morphology. Furthermore, the inter-planar distance d for all the samples is less than 0.326 nm.

FTIR spectra of melamine, intermediate product (rods), msg-C_3N_4 and g-C_3N_4 are shown in Fig. S5†. The peaks in the range of 3300–3500 cm^{-1} are assigned to the stretching vibration modes of NH and NH_2 groups and are observed in all the samples.[38,39] The absorption peaks from 800 cm^{-1} to 1400 cm^{-1} related to the breathing mode of s-triazine, amorphous sp^3 C–C bonds and C–N are also examined in all the samples; these results are consistent with the XRD and XPS results of msg-C_3N_4.[15,30] The peak at 1697 cm^{-1} is only present in the nanorods because of the existence of C=O bonds.[40] The presence of C=O plays a critical role in the formation of msg-C_3N_4. This C=O is only formed when melamine is pre-treated with HNO_3 in the presence of ethylene glycol. In the absence of HNO_3 or ethylene glycol this C=O is not formed, due to which the msg-C_3N_4 is also not achieved as discussed above.

PL studies were carried out at room temperature to study the bandgap of the synthesized materials (g-C_3N_4 and msg-C_3N_4) as shown in Fig. 4(a). UV light of 325 nm wavelength was used to excite the materials. The broad peak of msg-C_3N_4 and g-C_3N_4 at 427.6 and 452 nm, respectively, correspond to the bandgap of the respective samples. The bandgap of msg-C_3N_4 was calculated to be 2.9 eV as compared to 2.72 eV of g-C_3N_4. This is due to perfect packing and

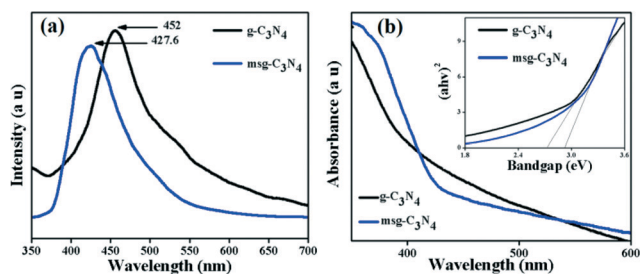Fig. 2 XPS spectra of msg-C_3N_4: (a) C1s, (b) N1s.

Fig. 4 (a) PL spectra of msg-C$_3$N$_4$ and g-C$_3$N$_4$; (b) UV spectrum of msg-C$_3$N$_4$ and g-C$_3$N$_4$ along with their bandgap (inset).

electronic coupling between the layers of single and non-connected msg-C$_3$N$_4$ and quantum confinement effects that shift conduction and valence band edges in opposite directions.[40,41] Therefore, it is believed that the bandgap with high energy level would acquire thermodynamically improved reduction and oxidation power in photodegradation of dyes. The charge-transfer rate between msg-C$_3$N$_4$ and redox species in solution also depends on these energy level relation.[40] Also, the PL intensity of msg-C$_3$N$_4$ is strong in comparison to g-C$_3$N$_4$, which indicates that the msg-C$_3$N$_4$ can be used as light-emitting material with high fluorescence quantum yield.[42,43] In order to further confirm the bandgap, UV studies were carried out. The UV spectra of msg-C$_3$N$_4$ and g-C$_3$N$_4$ along with their corresponding bandgaps are shown in Fig. 4(b). The bandgap of msg-C$_3$N$_4$ is 2.9 eV and the bandgap of g-C$_3$N$_4$ is 2.72 eV, in good agreement with the PL studies.

The surface area of the samples was calculated with the Brunauer–Emmett–Teller (BET) method in the relative pressure range of 0–1 by using 3H-2000PS2, China. The msg-C$_3$N$_4$ has a large surface area of 290 m^2 g^{-1} as compared to 10 m^2 g^{-1} for g-C$_3$N$_4$. The surface area of msg-C$_3$N$_4$ is 29 times greater than that of g-C$_3$N$_4$, which can also be observed from Fig. S7†. Thus, because of its large surface area msg-C$_3$N$_4$ provides more photocatalytic reaction sites for the adsorption of reactant molecules and increases the efficiency of the electron–hole separation, so the photocatalytic activity of msg-C$_3$N$_4$ is enhanced. Moreover, this large surface area also makes msg-C$_3$N$_4$ a promising candidate for hydrogen production.[8]

Photocatalytic performance of msg-C$_3$N$_4$

The photocatalytic activity of the msg-C$_3$N$_4$ was evaluated by degradation of RhB, MO and MB under visible light (wavelength >420 nm) irradiation in order to demonstrate its potential application for wastewater treatment. For the degradation of RhB, different amounts (10 mg, 20 mg, 50 mg and 100 mg) of msg-C$_3$N$_4$ and g-C$_3$N$_4$ were taken to explore the effect of concentration of photocatalysts upon RhB degradation. Fig. S12† shows the relationship between C/C_0 and time (C_0 is the initial concentration of the RhB, C is the concentration at time t) of all samples and for comparison a primary solution was irradiated without

catalyst under visible light. The sample without catalyst does not show any appreciable changes with time.[7,9]

Fig. 5(a) shows the relationship between C/C_0 and time for RhB, MB and MO with 100 mg concentration of msg-C$_3$N$_4$ and g-C$_3$N$_4$. The msg-C$_3$N$_4$ took just 45 minutes to completely degrade RhB whereas g-C$_3$N$_4$ required 75 minutes for complete degradation of RhB and a linear decrease in C/C_0 with time was observed. Similarly, the msg-C$_3$N$_4$ needed only 60 minutes for complete degradation of MB whereas g-C$_3$N$_4$ required 120 minutes for the same. Also for MO, msg-C$_3$N$_4$ took 165 minutes as compared to g-C$_3$N$_4$ which needed 270 minutes for complete degradation of the dye (Fig. S8–S13†). Fig. 5(b) shows the first order rate constant k (min^{-1}) of msg-C$_3$N$_4$ and g-C$_3$N$_4$ for RhB, MB and MO, which was calculated by the following first order equation:

$$\ln(C_0/C = kt)$$

where C_0 is the initial concentration of the dye in solution and C is the concentration of dye at time t. k has maximum value of 0.0372 min^{-1} for RhB when msg-C$_3$N$_4$ is used as a catalyst and it decreased to 0.0217 min^{-1} in the case of g-C$_3$N$_4$. Furthermore, it is 0.03336 min^{-1} for msg-C$_3$N$_4$ of MB and 0.0185 min^{-1} for g-C$_3$N$_4$. It also showed the improved performance for MO in the case of msg-C$_3$N$_4$ as compared to g-C$_3$N$_4$. In Table S1,† k values of carbon nitride and TiO$_2$ are given for comparison, which confirms that the msg-C$_3$N$_4$ is a more effective photocatalyst. Fig. S14† shows k (min^{-1}) of msg-C$_3$N$_4$ and g-C$_3$N$_4$ for RhB with different amount of samples. The msg-C$_3$N$_4$ with mass 50 mg has maximum k = 0.06603 min^{-1}, which was almost double that of g-C$_3$N$_4$. The formation of C=O bonds in the intermediate state leads to the novel structure of msg-C$_3$N$_4$, which is highly useful for a higher value of k (min^{-1}). The presence of small beads on the surface of micro strings, which extend their network deep into the strings (as suggested by SEM and BET), act as the reaction sites for the photocatalytic activity. Also, the small particle size of g-C$_3$N$_4$ tends to agglomerate into large particles, resulting in a poor photocatalytic performance of g-C$_3$N$_4$ as compared to msg-C$_3$N$_4$.

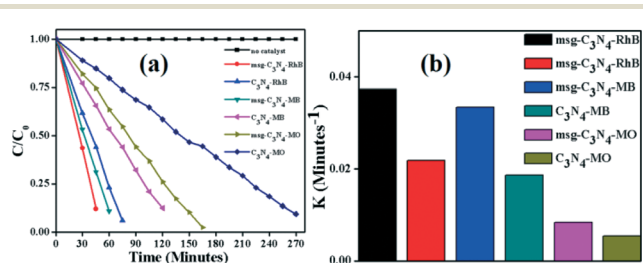The stability and reproducibility of the photocatalysts is highly important for its practical applications. In this context,

Fig. 5 (a) C/C_0 of msg-C$_3$N$_4$ and g-C$_3$N$_4$ for RhB, MB and MO. (b) First order rate constant k (min^{-1}) of msg-C$_3$N$_4$ and g-C$_3$N$_4$ for RhB, MB and MO.
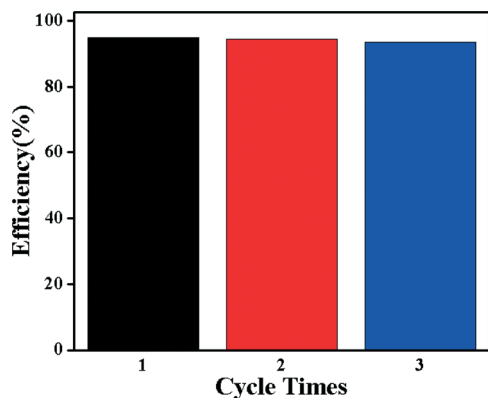
Fig. 6 Stability test of msg-C$_3$N$_4$ over three consecutive cycles.

the stability test of msg-C$_3$N$_4$ was performed by reusing the same catalyst for a second time for the degradation of organic dyes under similar conditions. It was observed that upon reusing the material for several cycles, the performance of material remains same and there is no significance loss in efficiency, as shown in Fig. 6. The degradation efficiency of msg-C$_3$N$_4$ decreased only 2% after three successive cycles, which indicates good stability and reusability of msg-C$_3$N$_4$ for several cycles without loss in activity at a pilot scale. The reactive nature of msg-C$_3$N$_4$ towards the photocatalytic reaction comes from the availability of photogenerated electrons for superoxide radical generation. The tailored bandgap and light of an appropriate wavelength generate these electrons needed for the oxidation reaction.[44]

The photocatalytic activity of msg-C$_3$N$_4$ is increased because of a positive shift in first order constant k as a result of H$_2$O$_2$ addition (Table S2†). Therefore, H$_2$O$_2$ increases the rate of hydroxyl radical production e.g. H$_2$O$_2$ + e → OH + OH$^-$ and enhances the efficiency of msg-C$_3$N$_4$.[45] Also, a large surface area and higher aspect ratio provides more reactive sites for reaction, which further polishes the photodegradation efficiency of msg-C$_3$N$_4$. It reduces the recombination probability of photoexcited charge carriers and enhances the transport of charges.[23–29]

Conclusions

In summary, a facile, green and economical approach has been designed to synthesize novel msg-C$_3$N$_4$. msg-C$_3$N$_4$ exhibits higher potential for application as a visible light photocatalyst for degradation of organic pollutants. These studies indicate that novel msg-C$_3$N$_4$ with high surface area and large aspect ratio can also be used for hydrogen production since it can provide more reactive sites. It reduces the recombination probability of photoexcited charge carriers and also increases the transport of charges. Strong PL intensity indicates that msg-C$_3$N$_4$ can be used as light-emitting materials. We anticipate that the msg-C$_3$N$_4$ will provide broad applications in the fields of photodetectors, field-effect

transistors, optical waveguides, drug delivery, lithium-ion batteries, electro catalysts and light-emitting materials.

Notes and references

1 M. R. Hoffmann, S. T. Martin, W. Choi and D. W. Bahnemann, *Chem. Rev.*, 1995, **95**, 69.
2 Y. Li, T. Sasaki, Y. Shimizu and N. Koshizaki, *J. Am. Chem. Soc.*, 2008, **130**, 14755.
3 X. Xiao and W. D. Zhang, *J. Mater. Chem.*, 2010, **20**, 5866.
4 D. M. Dalton and T. Rovis, *Nat. Chem.*, 2010, **2**, 710.
5 T. Yao, T. Cui, X. Fang, F. Cuia and J. Wu, *Nanoscale*, 2013, **5**, 5896.
6 X. C. Wang, K. Maeda, A. Thomas, K. Takanabe, G. Xin, J. M. Carlsson, K. Domen and M. Antonietti, *Nat. Mater.*, 2009, **8**, 76.
7 S. C. Yan, Z. S. Li and Z. G. Zou, *Langmuir*, 2010, **26**, 3894.
8 G. Liu, P. Niu, C. H. Sun, S. C. Smith, Z. G. Chen, G. Q. Lu and H. M. Cheng, *J. Am. Chem. Soc.*, 2010, **132**, 11642.
9 S. C. Yan, Z. S. Li and Z. G. Zou, *Langmuir*, 2009, **25**, 10397.
10 L. Ge, C. C. Han, J. Liu and Y. F. Li, *Appl. Catal., A*, 2011, **410**, 215.
11 Y. Wang, J. Yao, H.-R. Li, D. S. Su and M. Antonietti, *J. Am. Chem. Soc.*, 2011, **133**, 2362.
12 Y. Zheng, Y. Jiao, J. Chen, J. Liu, J. Liang, A. J. Du, W. M. Zhang, Z. H. Zhu, S. C. Smith, M. Jaroniec, G. Q. Lu and S. Z. Qiao, *J. Am. Chem. Soc.*, 2011, **133**, 20116.
13 K. Maeda, M. Higashi, D. Lu, R. Abe and K. Domen, *J. Am. Chem. Soc.*, 2010, **132**, 5858.
14 S. C. Yan, S. B. Lv, Z. S. Li and Z. G. Zou, *Dalton Trans.*, 2010, **39**, 1488.
15 L. Ge, C. C. Han and Liu, *Appl. Catal., B*, 2011, **108**, 100.
16 Y. Wang, R. Shi, J. Lin and Y. Zhu, *Energy Environ. Sci.*, 2011, **4**, 2922.
17 Y. J. Zhang, T. Mori, L. Niu and J. H. Ye, *Energy Environ. Sci.*, 2011, **4**, 4517.
18 W. H. Shin, S. H. Yang, Y. J. Choi, H. M. Jung, C. O. Song and J. K. Kang, *J. Mater. Chem.*, 2009, **19**, 4505.
19 X. C. Wang, K. Maeda and X. F. Chen, *J. Am. Chem. Soc.*, 2009, **131**, 1680.
20 Y. J. Zhang, A. Thomas, M. Antonietti and X. C. Wang, *J. Am. Chem. Soc.*, 2009, **131**, 50.
21 X. J. Wang, H. Pang, S. Zhao, W. Shao, B. Yan, X. Li, S. Li, J. Chen and W. Du, *ChemPhysChem*, 2013, **14**, 2518.
22 H. Pang, F. Gao and Q. Lu, *CrystEngComm*, 2010, **12**, 406.
23 F. Idrees, C. Cao, F. K. Butt, M. Tahir, M. Tanveer, I. Aslam, Z. Ali, T. Mahmood and J. H. Hou, *CrystEngComm*, 2013, **15**, 8146.

24 F. Dong, Z. Wanga, Y. Sun, W.-K. Ho and H. Zhang, *Colloidal Material and Nanomaterials*, 2013, vol. 401, 70.

25 L. Ge, C. Han, X. Xiao and L. Guo, *Appl. Catal., B*, 2013, **142**, 414.

26 L. Zhu, W. D. Zhang, C. H. Chen, B. Xu and M. F. Hou, *J. Nanosci. Nanotechnol.*, 2011, **11**, 4948.

27 J. Xu, Y. Li, S. Peng, G. Lu and S. Li, *Phys. Chem. Chem. Phys.*, 2013, **15**, 7657.

28 Y. Cui, J. Zhang, G. Zhang, J. Huang, P. Liu, M. Antonietti and X. C. Wang, *J. Mater. Chem.*, 2011, **21**, 13032.

29 J. Hong, X. Xia, Y. Wang and R. Xu, *J. Mater. Chem.*, 2012, **22**, 15006.

30 S. C. Lee, H. O. Lintang and L. Yuliati, *Chem.–Asian J.*, 2012, **7**, 2139.

31 Q. Lv, C. Cao, C. Li, J. Zhang, H. Zhu, X. Kong and X. Duan, *J. Mater. Chem.*, 2003, **13**, 1241.

32 M. Tahir, C. Cao, F. K. Butt, F. Idrees, N. Mahmood, Z. Ali, I. Aslam, M. Tanveer, M. Rizwan and T. Mahmood, *J. Mater. Chem. A*, 2013, **1**, 13949.

33 L. W. Yin, Y. Bando, M. S. Li, Y. X. Liu and Y. X. Qi, *Adv. Mater.*, 2003, **15**, 1840.

34 M. R. Wixom, *J. Am. Ceram. Soc.*, 1990, **73**, 1973.

35 X. Bai, C. Cao and X. Xu, *Mater. Sci. Eng.: B*, 2010, **175**, 95.

36 H. Z. Zhao, X. L. Chen, C. C. Jia, T. Zhou, X. H. Qu, J. K. Jian and Y. P. Xu, *Mater. Sci. Eng., B*, 2005, **122**, 90.

37 Q. Lv, C. B. Cao, C. Li, J. T. Zhang, H. S. Zhu, X. Kong and X. F. Duan, *J. Mater. Chem.*, 2003, **13**, 1241.

38 X. Bai, J. Li and C. Cao, *Appl. Surf. Sci.*, 2010, **256**, 2327.

39 J. Gao, Y. Zhou, Z. Li, S. Yan, N. Wang and Z. Zou, *Nanoscale*, 2012, **4**, 3687.

40 Y. C. Zhao, Z. Liu, W. G. Chu, L. Song, Z. X. Zhang, D. L. Yu, Y. J. Tian, S. S. Xie and L. F. Sun, *Adv. Mater.*, 2008, **20**, 1777.

41 M. Hu, J. Reboul, S. Furukawa, L. Radhakrishnan, Y. Zhang, P. Srinivasu, H. Iwai, H. Wang, Y. Nemoto, N. Suzuki, S. Kitagawa and Y. Yamauchi, *Chem. Commun.*, 2011, **47**, 8124.

42 K. Suenaga, M. Yudasaka, C. Colliex and S. Iijima, *Chem. Phys. Lett.*, 2000, **316**, 365.

43 P. Niu, G. Liu and H.-M. Cheng, *J. Phys. Chem. C*, 2012, **116**, 11013.

44 M. Lee, C. Liao, C. Tsai and C. Chen, *Adv. Mater.*, 2005, **17**, 2493.

45 Y. S. Jun, E. Z. Lee, X. Wang, W. H. Hong, G. D. Stucky and A. Thomas, *Adv. Funct. Mater.*, 2013, **23**, 3661.